Published in final edited form as:
J Immunol. 2005 February 15; 174(4): 2143–2151.

Electrostatic Modeling Predicts the Activities of Orthopoxvirus Complement Control Proteins[1]

Georgia Sfyroera[*], **Madan Katragadda**[*], **Dimitrios Morikis**[‡], **Stuart N. Isaacs**[†], and **John D. Lambris**[2,*]

[*]Department of Pathology and Laboratory Medicine, University of Pennsylvania School of Medicine, Philadelphia, PA 19104

[†]Department of Medicine, Division of Infectious Diseases, University of Pennsylvania School of Medicine, Philadelphia, PA 19104

[‡]Department of Chemical and Environmental Engineering, University of California, Riverside, CA 92521

Abstract

Regulation of complement activation by pathogens and the host are critical for survival. Using two highly related orthopoxvirus proteins, the vaccinia and variola (smallpox) virus complement control proteins, which differ by only 11 aa, but differ 1000-fold in their ability to regulate complement activation, we investigated the role of electrostatic potential in predicting functional activity. Electrostatic modeling of the two proteins predicted that altering the vaccinia virus protein to contain the amino acids present in the second short consensus repeat domain of the smallpox protein would result in a vaccinia virus protein with increased complement regulatory activity. Mutagenesis of the vaccinia virus protein confirmed that changing the electrostatic potential of specific regions of the molecule influences its activity and identifies critical residues that result in enhanced function as measured by binding to C3b, inhibition of the alternative pathway of complement activation, and cofactor activity. In addition, we also demonstrate that despite the enhanced activity of the variola virus protein, its cofactor activity in the factor I-mediated degradation of C3b does not result in the cleavage of the α′ chain of C3b between residues 954–955. Our data have important implications in our understanding of how regulators of complement activation interact with complement, the regulation of the innate immune system, and the rational design of potent complement inhibitors that might be used as therapeutic agents.

Members of the family of regulators of complement activation (RCA)[3] are critical proteins that help prevent complement-mediated damage to the host (1). These proteins contain

[1]This work is supported by National Institutes of Health Grants AI48487, AI47237, and AI30040.

[2]Address correspondence and reprint requests to Dr. John D. Lambris, Protein Chemistry Laboratory, Department of Pathology and Laboratory Medicine, 401 Stellar-Chance Laboratories, 422 Curie Boulevard, University of Pennsylvania, Philadelphia, PA 19104. lambris@mail.med.upenn.edu.

[3]Abbreviations used in this paper: RCA, regulator of complement activation; SCR, short consensus repeat; CR1, complement receptor 1; C4bp, C4-binding protein; VCP, vaccinia virus complement control protein; Fc, flow cell; SPICE, smallpox inhibitor of complement enzymes; GVB, gelatin veronal-buffered saline; SPR, surface plasmon resonance; PDB, Protein Data Bank.

multiple structural and functional domains known as short consensus repeats (SCRs). These SCR domains are ˜60-to 70-aa in length and contain highly conserved cysteines that form two intramolecular disulfide bonds within an SCR (2, 3). Members of this family, like factor H, complement receptor 1 (CR1), membrane cofactor protein, decay accelerating factor protein, and C4-binding protein (C4bp), have 4–30 SCRs that tightly control the balance between the activated and the nonactivated forms of C3.

Insights into how these RCA proteins interact with complement can be attained by studying SCR-containing proteins encoded by simpler organisms. Viruses have developed several strategies to defend against the host complement-mediated attack (4–6). Orthopoxviruses encode a secreted protein that has four SCR domains with significant homology to members of the RCA (7). The most studied orthopoxvirus complement binding protein is the vaccinia virus complement control protein (VCP). This 263-aa protein shares 38% homology to the first half of C4bp and 35 and 31% with membrane cofactor protein and decay accelerating factor protein, respectively (8). VCP is secreted by vaccinia virus-infected cells, inhibits complement activation, and is a virulence factor (9,10). VCP prevents the activation of the classical and alternative pathway C3 convertases and accelerates their decay (11–14). Furthermore, it inhibits complement activation by binding to C3b/C4b and acts as a cofactor in the factor I-mediated enzymatic inactivation of C3b/C4b (11–15). The structure of VCP has been solved by nuclear magnetic resonance spectroscopy and protein crystal-lography (16–20). Recently, the VCP homologue present in variola virus, the causative organism of smallpox, was expressed and studied (21). The variola homologue, named smallpox inhibitor of complement enzymes (SPICE), differs from VCP by only 11 aa residues. All of the amino acid differences are distributed along SCR-2, -3, and -4. Rosengard et al. (21) showed that SPICE possesses factor I cofactor activity for inactivating C3b and C4b and demonstrated that SPICE is ˜100-fold more potent than VCP at inactivating C3b and 6-fold more efficient at inactivating C4b.

Here we propose and experimentally test a model based on the electrostatic predictions of the interaction of two viral proteins with C3b; the predictions illustrate how certain residue changes result in enhanced activity of SPICE. We also demonstrate that despite this enhanced activity, SPICE cofactor activity in the factor I-mediated degradation of C3b does not result in the cleavage of the α′ chain of C3b between residues 954–955.

Materials and Methods

Cloning of VCP and site-directed mutagenesis

Recombinant and mutated forms of VCP were expressed using the *Escherichia coli* pQE30 expression system (Qiagen). The PCR oligonucleotide primers used to amplify the 732-bp DNA fragment of the C3L ORF of the vaccinia virus (strain WR) (22) that encodes the naturally secreted portion of VCP were 5′-AATGGATCCTGCTGTACTATTCCGTCACGA-3′ (the *Bam*HI site is underlined) and 5′-GGCAAGCTTTCAGCGTACACATTTTGGAAGTTC-3′ (the *Hind*III site is underlined and the stop codon is in boldface). The product generated after 30 cycles of 95°C for 1 min, 56°C for 1 min, and 72°C for 1 min was gel purified, digested with *Bam*HI and *Hind*III, and

ligated into the similarly cut pQE30 plasmid. The DNA sequence was confirmed by sequencing.

For the generation of a panel of mutated VCPs, the nucleotide sequence of VCP was mutated using the QuikChange Multi Site-Directed Mutagenesis kit (Stratagene). The positions (Fig. 1A) that were changed are the following: CAA77CAT, CAT98TAT, TCT103TAT, GAA108AAA, GAG120AAG, TCC131TTG, GAG144AAT, GAT178AAT, TCA193TTA, AAG214ACG, and AAG236CAG (the first codon represents the nucleotide triplet on VCP; the number identifies the position of the amino acid; and the second triplet corresponds to the sequence of SPICE). The DNA sequences of the mutated plasmids were confirmed twice by sequencing of both strands. As shown in Fig. 1B, the proteins VCP-SPICE2, VCP-SPICE3, and VCP-SPICE4 have the parental sequence of VCP and the indicated SCR representing the SPICE sequence. For example, the protein VCP-SPICE2 comprises SCR-1, -3, and -4 of VCP and SCR-2 of SPICE. Mutants containing only single- or double-residue mutations are represented by the amino acid name, number, and amino acid substitution (Fig. 1B).

Expression and purification of recombinant proteins

The DNA plasmids were used to transform M15 competent cells and a single colony was inoculated in 5 ml of SOB medium (0.5% yeast extract, 2.0% tryptone, 10 mM NaCl, 2.5 mM KCI, and 10 mM $MgCl_2$). This overnight culture was then inoculated into 1 liter of SOB medium, incubated at 37°C, and grown to OD_{600} 0.6–0.9. Protein expression was then induced by adding 1 mM isopropylthio-β-D-galactoside and allowing further incubation for 4 additional hours. The cell pellets were stored at −70°C or they were processed for purification immediately.

The purification of the recombinant proteins was performed following standard procedures (23). Briefly, frozen cell pellets were washed twice with 50 mM Tris/50 mM NaCl/1 mM EDTA/0.1 mM PMSF, pH 8.0, and then sonicated with 10 pulses of 10 s each. The samples were centrifuged, and the pellets containing inclusion bodies were washed three times with the aforementioned buffer. The pellets were solubilized by suspending them in buffer comprised of 0.2 M Tris/8 M urea/0.05 M 2-ME/1 mM EDTA, pH 8.5, and left static for 1 h atroom temperature. Following the solubilization of the inclusion bodies, SP-Sepharose FF (Pharmacia), equilibrated in the same buffer, was added and incubated for 1 h with rotation. This material was then packed into a column, washed with the aforementioned buffer, and the proteins were eluted with high concentrations of salt. To achieve proper folding of the recombinant proteins (23), the protein was rapidly diluted into buffer containing 0.02 M ethanolamine/1 mM EDTA/0.5 mM oxidized glutathione/reduced glutathione and left static at 4°C for 2–3 days. The solution was then concentrated using a 10-kDa molecular mass cut off membrane and the protein purified using a Hi-Trap heparin column (Amersham Biosciences) (19). At the end of the purification procedures, the protein was dialyzed against PBS, pH 7.4, and the purity of the proteins was assessed by SDS-PAGE and mass spectrometry.

Circular dichroism (CD)

CD measurements were performed using a Jasco 810 spectropolarimeter with a cylindrical quartz cell with a path length of 0.01 cm. Measurements were taken at 25°C in 10 mM phosphate buffer, pH 7.0, using 0.2 mg/ml protein concentration for VCP, 0.4 mg/ml for SPICE, 0.04 mg/ml for VCPE108K/E120K, and 0.65 mg/ml for VCP-SPICE2. All the data were subtracted against the background data using the spectral analysis software.

Factor I cofactor activity of VCP mutants

The cleavage of human C3b by factor I in the presence of VCP and VCP-SPICE mutants, was performed in 10 mM phosphate buffer, pH 7.4, containing 150 mM NaCl. Specifically, 500 ng of C3b were mixed with 300 ng of VCP or its mutants and 10 ng of factor I in a total volume of 20 μl. The samples were incubated at 37°C and at different time points samples were mixed with loading buffer containing mercaptoethanol, boiled for 5 min, and subjected to electrophoresis on a 9% SDS-PAGE gel. The proteins were transferred to a polyvinylidene difluoride membrane, blocked with 10% milk in PBS for 1 h at 25°C, and then probed with rabbit polyclonal anti-C3b (diluted 1/5000 in 10% milk-PBS containing 0.005% Tween 20) for 1 h at 25°C. This anti-C3b Ab recognizes all C3b breakdown products including C3dg. After the membrane was washed twice for 15 min in PBS-0.005% Tween 20, the degradation products of C3b were detected with HRP-conjugated goat anti-rabbit Ab for 30 min at 25°C, and bands were visualized by chemiluminescence according to the manufacturer's instructions.

Inhibition of classical pathway complement activation by VCP or its mutants

The ability of VCP and its mutants to modulate complement activation through the classical pathway was evaluated using an ELISA-based assay. Ninety-six-well ELISA plates were coated with 50 μl of 1% chicken OVA in PBS for 2 h at room temperature. After coating, wells were blocked with 200 μl of 1% BSA/PBS. To form an immunocomplex on the plate, polyclonal anti-chicken OVA Ab was added to the wells at a final concentration of 1/1000. Following a 1-h incubation, VCP or its mutants were serial diluted in GVB^{++} and added to each well. GVB^{++} was gelatin veronal-buffered saline (GVB; veronal-buffered saline, pH 7.4, 5 mM barbital, 145 mM NaCl, 0.1% gelatin) containing 0.5 mM $MgCl_2$ and 0.15 mM $CaCl_2$. Then a 1/80 dilution of human plasma (collected in 50 μg/ml lipirudin) in the same buffer was added to the wells and the mixture was incubated at room temperature for 1 h. Detection of C3b bound in wells was performed using a 1/1000 dilution of anti-human C3 HRP-conjugated Ab (ICN Cappel). After washes with PBS containing 0.005% Tween 20, color was developed by adding ABTS peroxidase substrate, and OD was measured at 405 nm. The percent inhibition was plotted against the protein concentration and the resulting data set was fit to a logistic dose-response function using Origin 7.0 software (OriginLab Corporation). IC_{50} values were obtained from the fit parameters that achieved the lowest χ^2 value.

Inhibition of alternative pathway complement activation by VCP or its mutants

The ability of VCP and its mutants to modulate the alternative pathway complement activation was similarly evaluated using an ELISA-based assay that used LPS as the

complement activator (24). Ninety-six-well ELISA plates were coated with 40 μg/ml LPS from *Salmonella typhosa* in PBS for 2 h at room temperature. After coating, wells were blocked with 200 μl of 1% BSA for 1 h, and VCP or its mutants were serial diluted in GVB-MgEGTA (GVB containing 0.1 M $MgCl_2$ and 0.1 M EGTA) and added to the wells. Human serum in the same buffer at a final concentration of 1/10 was then added to each well and incubated for 1 h. To detect C3b bound to the wells, a 1/1000 dilution of anti-human C3 HRP-conjugated Ab (ICN Cappel) was used. After washes with PBS containing 0.005% Tween 20, color was developed by adding ABTS peroxidase substrate, and OD was measured at 405 nm. IC_{50} values were obtained as described above.

Direct binding of VCP and its mutants to C3b

The relative binding of VCP and the various VCP-mutants to C3b was determined by surface plasmon resonance (15, 25). The BIAcore was only used to determine the relative binding of various VCP mutants to C3b and not to determine the kinetics of their interactions. All the experiments were performed using the biosensor BIAcore × (BIAcore). The experiments were performed at 25°C in PBS containing 0.05% Tween 20 (pH 7.4) at physiological ionic strength (150 mM NaCl). To orient ligand onto the chip, C3b was biotinylated at a specific residue as previously described (25) and then immobilized on a streptavidin chip (Sensor Chip SA; BIA-core) to a reading of 2040 resonance response units on flow cell-2 (Fc2). Flow cell-1 (Fc1) was used as a blank control. The binding was measured at 10 μl/min. A baseline was established, and then 50 nM of analyte (VCP or VCP-mutants) was injected and the association was followed for 120–300 s. The relative binding of the proteins to immobilized C3b was monitored by observing the binding response of analyte throughout the experiment. Regeneration was achieved by injecting 20 μl of 1 M NaCl. Biosensor data for the control Fc1 were subtracted from those obtained for the immobilized protein. BIAevaluation 3.0 (BIAcore) software was used to analyze the binding data.

Electrostatic calculations

Computational modeling was performed using the program Swiss-Pdb-Viewer (26). The Protein Data Bank (PDB; Ref. 27) structure of VCP with PDB code 1g40 (19) was used as the template for our calculations. The structure 1g40 comprises a dimer. For our calculations, monomer 2 (chain B) was removed and monomer 1 (chain A) was retained. Theoretical mutations and calculations of electrostatic potentials were performed with Swiss-PdbViewer (26). After each theoretical mutation, 20 steps of steepest descent energy minimization was performed in vacuo, using the GROMOS96 force field implementation of Swiss-PdbViewer. Simple Coulomb's Law with single dielectric constant of 80 and without partial charges was used to calculate electrostatic potentials. The protein pH was considered to be 7.0, with lysine and arginine residues being positively charged and aspartic acid and glutamic acid residues being negatively charged.

Results

Expression and characterization of VCP and SPICE

VCP differs from SPICE by 11 aa that vary in their acidic-basic and hydrophobic-polar nature (Fig. 1A). We introduced these 11 aa changes into VCP and expressed both VCP and the resulting SPICE using an *E. coli* expression system. VCP and SPICE ran as a single band on a reducing SDS gel with the SPICE protein migrating slightly faster (Fig. 2B). On Western blot, the bacterial produced VCP ran identical to VCP produced by vaccinia virus-infected cells (data not shown). To further characterize the recombinant proteins, mass spectrometric analysis was performed (Fig. 2A). As indicated in the figure, VCP and SPICE appeared with exact molecular weights of 28.247 kDa and 28.158 kDa, respectively. Because the proteins were produced in bacteria and required refolding to form the proper intramolecular disulfide bonds present in SCR domains, we examined the protein structure by CD spectroscopy. We found that the CD spectrum obtained for the *E. coli*-produced VCP was similar to the one published using the VCP expressed in yeast (17). Also, the secondary structure composition calculated using the CDSSTR algorithm of the DICHROWEB software (28, 29) agrees with the secondary structure composition calculated from the crystal structure. These findings provide assurance that the proteins assumed native conformation were correct following the refolding procedure. Fig. 2C shows the secondary structure composition calculated from deconvoluting the CD spectra obtained for VCP and SPICE (as well as VCP-SPICE2 and VCP-E108K/E120K). Interestingly, VCP and SPICE showed similar secondary structure compositions suggesting that both proteins have similar topology. In addition, the minimal changes observed in the secondary structure compositions observed upon single- and double-point mutations indicate that the secondary structure of VCP remains unchanged following these mutations.

Binding of VCP and SPICE to C3b and inhibition of complement activation

To compare the binding of VCP and SPICE with C3b, surface plasmon resonance (SPR) experiments were conducted. Biotinylated C3b was immobilized in an orientation-specific fashion on an SA chip (25), and then recombinant proteins at a concentration of 50 nM were passed through at 10 μl/min. As shown in Fig. 3A, SPICE had 25-times higher binding to C3b than VCP.

To dissect the specific involvement of VCP and SPICE at inhibiting different complement activation pathways, we performed assays that analyzed classical and alternative pathways of complement activation. We determined that the concentration of VCP and SPICE required to inhibit 50% of the classical pathway activity (IC_{50}) was 416 nM and 5 nM, respectively (Fig. 3B). Thus, SPICE was ˜75-times more active than VCP at inhibiting the classical pathway. In contrast, SPICE inhibited the alternative pathway with an IC_{50} value of 1.0 nM and VCP inhibited the alternative pathway with an IC_{50} of 1026 nM. This indicates that SPICE is ˜1000-times more potent as an inhibitor of the alternative pathway than VCP. These results support and extend the prior work that showed increased activity of SPICE vs VCP (21). Also as shown previously (11, 21, 30), VCP appears to be more active at inhibiting the classical pathway than inhibiting the alternative pathway. In contrast, SPICE

is ~5-times more active inhibiting the alternative pathway than inhibiting the classical pathway.

SPICE and VCP were evaluated for their potency as cofactors in the factor I-mediated degradation of C3b. As shown in Fig. 3C, the two proteins follow different kinetics of C3b cleavage. Within 5 min of incubation in the presence of SPICE, the α′ chain of human C3b was completely cleaved to a 43-kDa fragment, indicating the cleavage of C3b in two positions at 1320–1321 and 1303–1304. The factor I-mediated cleavage of C3b in the presence of VCP was much slower. The α′ chain disappeared only after 240 min of incubation. Importantly, longer incubation times in the presence of SPICE did not result in the appearance of the 41-kDa C3dg fragment of the α′ chain. Therefore, in contrast to previous observations (21), there is no indication that SPICE can support the cleavage of α′ chain on C3b at position 954–955.

Electrostatic modeling

Although the charge of individual residues have been implicated in the function of RCA proteins (31), we performed electrostatic modeling of VCP and SPICE to test the hypothesis that residue changes could have global affects that could explain the orders of magnitude difference in activity between the two highly related proteins. To test this possibility we used a three-dimensional crystallographic structure of VCP (19) to calculate electrostatic potentials (31). Fig. 4 shows the isoelectrostatic contour surfaces for VCP and for modeled structures of SPICE and several mutants. Isopotential contour surfaces are shown for positive charges (in blue) and for negative charges (in red). The orientation of the structures is identical in all panels, and the electrostatic calculations were performed in an identical manner. Fig. 4 shows that SCR-1 predominantly is charged positively in both VCP and SPICE, with SPICE possessing a stronger positive electrostatic potential. In VCP, the interface between SCR-2 and SCR-3 has strong negative electrostatic potential, which is nearly eliminated in SPICE. In both VCP and SPICE, SCR-4 has similar electrostatic character where positive and negative potentials nearly cancel out. Based on these observations and the higher inhibitory activity of SPICE compared with VCP, we formed and subsequently tested the following hypotheses: 1) increase of the positive electrostatic potential of SCR-1 produces increased activity, 2) reduction (or elimination) of the negative electrostatic potential of SCR-2/SCR-3 produces increased activity, or 3) both of the above. Indeed, hypotheses 1 and 2 are related, because decrease of the negative character of SCR-2/SCR-3 is responsible for increase of the positive character of SCR-1, owed to less charge cancellation. To test our hypotheses, we calculated the electrostatic potentials of a series of mutants (Fig. 4) and then constructed experimental mutants summarized in Fig. 1B.

Mapping of the SCRs of SPICE involved in the enhanced interaction of SPICE with C3b

To test whether the electrostatic models predicted the residues responsible for the overall higher activity of SPICE compared with VCP, we first tested mutants containing various combinations of altered SCRs (Fig. 5). Because SPICE and VCP-SPICE2 had similar electrostatic potentials (Fig. 4), we predicted that they would have similar activities when compared with each other and higher activities when compared with the other single SCR substitutions. We evaluated the direct binding of the different proteins to C3b using SPR

(Fig. 5A) and found VCP-SPICE2 binding to C3b was similar to that of SPICE. The kinetics of this binding was different from the binding of SPICE. VCP-SPICE2 has a slower association and dissociation rates compared with SPICE. In contrast, the proteins VCP-SPICE3 and VCP-SPICE4 bound to C3b with 6- and 5-times higher binding than VCP, respectively. We also modeled simultaneous substitutions of two SCRs and found that VCP-SPICE2–3 had similar electrostatic profile for SCR-1 and the interface of SCR-2/SCR-3 and similar activity to SPICE (Figs. 4 and 5 and data not shown).

All of the proteins were evaluated for their ability to inhibit the alternative pathway of complement activation (Fig. 5B). The amount of protein needed to inhibit the 50% of complement activation (IC_{50}) was 15, 424, and 279 nM for the proteins VCP-SPICE2, VCP-SPICE3, and VCP-SPICE4, respectively. All of the proteins appear to have lower activity than SPICE with relative ratios ranging from 5 to 140. The IC_{50} value of the mutant containing two SPICE SCRs (VCP-SPICE2–3) was 4 nM, similar to SPICE, suggesting that the eight mutations on these two SCRs are sufficient to make VCP as active as SPICE.

To measure the cofactor activity of the proteins, C3b degradation experiments were conducted in the presence of factor I. VCP-SPICE2 and VCP-SPICE4 showed a similar cleavage pattern as SPICE (Fig. 5C). The α' chain of C3b is cleaved within 5 min of incubation and the degradation products of 46 and 43 kDa appear on Western blot. Factor I/VCP-SPICE3-mediated degradation of C3b followed a slower degradation rate, resulting in the disappearance of α' chain only after 20 min of incubation.

The electrostatic models of VCP-SPICE2 and VCP-SPICE2–3 have SCR-1 modules with similar electrostatic potential (Fig. 4), while the strength of the negative electrostatic potential of their SCR-2/SCR-3 modules follows the order SPICE $\approx$ VCP-SPICE2– 3 < VCP-SPICE2. This is the order of binding and inhibitory activity, from higher to lower, we found (Fig. 5, A and B). VCP-SPICE2–3 has similar electrostatic potential at the SCR-2/SCR-3 interface as SPICE, but slightly different from VCP-SPICE2. In both VCP-SPICE2 and VCP-SPICE2–3 there is change in opposite charge cancellation between SCR-1 and SCR-2/SCR-3, resulting from the mutations in SCR-2 (Fig. 4). But, in the case of VCP-SPICE2–3 there is further change in charge cancellation, as seen by the enhanced positive charge of SCR-4, resulting from the mutations in SCR-3 (Fig. 4). This double cancellation makes the electrostatic potential of the SCR-2/SCR-3 interface of VCP-SPICE2–3 similar to that of SPICE.

Thus, we have formed a correlation between the reduction of the negative character of SCR-2/SCR-3 inhibitory activity. Reduction of the negative character occurs by the mutations of acidic amino acids in SCR-2 and SCR-3. From the remaining mutants, VCP-SPICE3 and VCP-SPICE4 more closely resemble VCP, but with variations in the positive character of SCR-1 and negative character of SCR-2/SCR-3. These three proteins show similar binding and inhibitory activities (Fig. 5, A and B).

Mapping of the complement modulating activity of VCP in SCR-2 by single-point mutations

Of all the SPICE single SCR domain substitutions, we found that the substitution of the SPICE SCR-2 in VCP resulted in a protein with an electrostatic profile most similar to

SPICE and with the most enhanced activity when compared with VCP. We thus generated single-amino-acid-point mutations in VCP (Fig. 1B) to correlate the electrostatic models of each amino acid substitution and the actual activity of the mutated protein. SPR experiments with the various proteins (Fig. 6A) showed a substantial increase of the C3b-binding for all the individual mutations that are present in SPICE SCR-2—S103Y, Q77H, H98Y, E108K and E120K—when compared with VCP. Each of these individual mutations in VCP had approximately the same binding to C3b. We then assessed each individual point mutation for its ability to inhibit the alternative pathway of complement activation (Fig. 6B). All the proteins appeared to have a considerable increase in their complement modulating activity when compared with VCP. VCP-E120K had an IC_{50} value of 15 nM, almost 87-times lower than VCP. VCP-H98Y had an IC_{50} of 48 nM (28-times lower than VCP); VCP-S103Y had an IC_{50} of 56 nM (24-times lower than VCP); VCP-E108K had an IC_{50} of 79 nM (17-times lower than VCP); and VCP-Q77H an IC_{50} of 122 nM (11-times lower than VCP). This further suggested the direct involvement of SCR-2 into the increased activity of SPICE.

Examination of the electrostatic potentials of the single mutations present in the SCR-2 module of SPICE (Fig. 4) predicted that mutants VCP-E108K and VCP-E120K would have the greatest activity. This was the case of the binding abilities and inhibitory activities of VCP-E108K and VCP-E120K as shown in Fig. 6. Because of the setup of our calculations, it is expected that VCP and VCP-Q77H, VCP-H98Y, and VCP-S103Y have identical electrostatic potentials. This is because in our Coulombic calculations, histidine and tyrosine have always been treated as neutral at pH 7 (see *Materials and Methods*). This is based on the assumption that the pK_a values of histidine and tyrosine are similar to their model pK_a values of free amino acids in solution: 6.3 and 9.6, respectively. However, this may not be the case in reality, and calculations to predict apparent pK_a values for each ionizable residue of VCP, followed by more rigorous electrostatic calculations using the predicted pK_a values may be needed. This calculation detail may explain the small increase in binding and inhibitory activities for VCP-Q77H, VCP-H98Y, and VCP-S103Y compared with VCP (Fig. 6).

Mapping of the inhibitory activity of SPICE by mutations at only positions E108K/E120K on VCP

Based on the electrostatic potential of the various amino acid changes in SPICE (Fig. 4), we predicted that a double mutation (E108K and E120K) introduced into VCP would be the minimal amino acid substitutions required on VCP to bring its activity close to the activity of SPICE. Thus, we expressed and evaluated the activity of the VCP-E108K/E120K. For the analysis of the binding of this molecule to C3b, SPR experiments were performed (Fig. 7A). As shown, VCP-E108K/E120K had about the same binding to C3b as VCP-SPICE2 suggesting the importance of these two positions for the binding of SPICE to C3b.

The activity of SPICE, VCP-E108K/E120K, and VCP-SPICE2 was tested for the ability to inhibit the alternative pathway of complement activation. VCP-E108K/E120K had an IC_{50} value of 3 nM; SPICE had an IC_{50} value of 3 nM; and VCP-SPICE2 had an IC_{50} value of 15 nM. These results underscore the critical role of amino acid residues E108 and E120 have in regulating the activity of VCP and confirm the electrostatic predications.

Examination of the electrostatic potentials of SPICE, VCPE108K/E120K, and VCP-SPICE2 (Fig. 4) shows subtle differences in the strength of the negative electrostatic potential of SCR-2/ SCR-3, in the order SPICE < VCP-E108K/E120K < VCP-SPICE2. This order correlates well with the order of binding (Fig. 7A) and is in excellent agreement with the order of inhibitory activity.

To evaluate the factor I cofactor activity of VCP-E108K/E120K we studied C3b degradation. The protein, in the presence of factor I, completely cleaved the α′ chain of C3b within 5 min, indicating a C3b degradation rate similar to SPICE (Fig. 7B). This again establishes the finding of the increased activity of VCP-E108K/ E120K and supports the electrostatic model of enhancement of complement regulatory activity of SCR-containing proteins.

Discussion

Our data demonstrate how the 11 residues that differ between SPICE and VCP result in such enhanced function. In our study, we expressed VCP, mutated versions of VCP, and SPICE using a prokaryotic *E. coli* system. Such an approach, which includes a protein-refolding step, has been successful for the expression of functional SCR-containing proteins (23). The characterization of our purified proteins indicated that they were folded correctly, and functional assays indicated that they had complement regulatory activity. We found that SPICE was 1000-times and 75-times more active then VCP at inhibiting the alternative and the classical pathways of complement activation, respectively. Therefore, we focused our work on investigating the effect of the mutated proteins on the alternative pathway of complement activation. Like the prior study with baculovirus expressed SPICE (21), we too found significant differences with the cofactor activity between VCP and SPICE. SPICE helped mediate a much faster rate of degradation of C3b. However, as opposed to the previous report that SPICE could support the cleavage of C3b at residues 954–955, which results in the generation of the fragment C3dg (21), we found products that would only result from two cleavages of the α′ chain of C3b at 1320–1321 and 1303–1304. This is an important finding because it supports current dogma that only CR1 has an efficient cofactor activity that leads to the cleavage of C3b at position 954–955 resulting in the formation of C3dg (32, 33). Similar to this prior report that SPICE, along with factor I, could mediate the formation of C3dg (21), the complement control protein encoded by the Kaposi's sarcoma-associated herpesvirus had at first been reported to mediate the formation of a C3d-product (34). However, recently the same group showed that this viral protein only acted as the cofactor in the formation of iC3b (35). This indicates an important difference in the cofactor activity of CR1 compared with all other SCR-containing complement regulatory proteins. We believe that the prior work with the viral complement regulatory proteins that showed formation of C3b cleavage products beyond the second cleavage were due to enhanced susceptibility of $iC3b_2$ to nonspecific proteases that may have been present in the reaction mix. Because SPICE is not glycosylated, we do not think the differences we found were due to the fact that our protein was produced in bacteria, while the prior study expressed SPICE in baculovirus.

The three-orders-of-magnitude increase in the complement regulatory activity of SPICE when compared with VCP permitted the systematic study of the domains and amino acid changes that contributed to this enhanced activity predicted by electrostatic modeling. Although the amino acid sequence of SCR-1 was identical between VCP and SPICE, SCR-2 contained five residue changes and SCR-3 and -4 each had three residue differences. The crystal structure of VCP has been previously solved (19) and showed that each of the four SCR modules fold into a compact 6- to 8-stranded β-structure. All of the amino acid substitutions that convert VCP to SPICE appear to be on the surface of the molecule (21). The presence of these amino acid substitutions on the molecular surface was an indication that they do not substantially alter the folding of the protein, for which the amino acids of the predominantly hydrophobic protein core are responsible. This was also demonstrated experimentally because the CD spectra (Fig. 2C) of VCP and SPICE were similar, indicating similar conformations of the proteins.

We hypothesized that the differences in the activity observed could be due to the changes in electrostatic potentials of the proteins. Indeed, our electrostatic modeling of VCP and SPICE (Fig. 4) showed that the VCP electrostatic potential appears to be positive around SCR-1 and negative around the linker area of SCR-2 and SCR-3. In contrast, SPICE appears to have more positive charge around SCR-1 and less negative charge in the SCR-2/SCR-3 linker (Fig. 4). Thus, our data and these electrostatic observations suggest a Coulombic-type interaction between VCP/SPICE and C3b. That is, recognition between VCP or SPICE and C3b occurs through long-range electrostatic attraction. This hypothesis was supported by the modeling of the electrostatic potentials and activity of VCP, SPICE, VCP-SPICE2, VCP-SPICE3, VCP-SPICE4, VCP-SPICE2–3, VCP-E108K, and VCP-E120K.

We found that substituting the combination of SCR-2 and SCR-3 from SPICE in VCP (VCP-SPICE2–3) had C3b-binding, alternative pathway-regulatory activity, and cofactor activity nearly identical to SPICE. Examination of the electrostatic potential of VCP-SPICE2–3 suggested that reduction of negative charge by mutations of acidic amino acids in SCR-2 and SCR-3 resulted in enhanced positive electrostatic potential not only in SCR-1 but also in SCR-2. Although other combinations of SCR substitutions enhanced activity when compared with VCP, they were not as active as the SCR 2–3 substitution (data not shown). The most dramatic single SCR substitution was with SPICE SCR-2 (VCP-SPICE2). This protein was 148-times more active at regulation than VCP, and only 5-fold less active than SPICE. VCP-SPICE3 and VCP-SPICE4 showed 5.2- and 7.8-fold higher activity, respectively, than VCP at inhibiting the alternative pathway activation.

In general, binding experiments of the mutated proteins with C3b showed increased binding to the ligand that correlated with the observed inhibition of the alternative pathway. For example, VCP-SPICE2, the most active protein with a single SCR substitution, bound C3b with similar level of binding as seen with SPICE, although the kinetics of C3b binding was different from SPICE (Fig. 5A). Cofactor experiments conducted in the presence of VCP-SPICE2, VCP-SPICE3 and VCP-SPICE4 recombinant proteins showed clearly that amino acid substitutions on SCR-2 and SCR-4 on VCP increase the rate of C3b cleavage dramatically. Interestingly, VCP-SPICE4 appeared to have less binding ability to C3b than VCP-SPICE3, yet its inhibition of alternative pathway and its cofactor activity was

significantly higher. This is somewhat similar to what has been described for C4bp (36) (and CR1 (37)). The cofactor activity and the binding site of C4bp to C3b can be localized to different sites on the molecule, meaning that these two activities are separable. Based on our studies of VCP containing various SPICE SCRs, we believe that this is also the case for this viral complement regulatory protein. The C3b binding activity of SPICE mainly involves residues located in SCR-2 and SCR-3 while the factor I cofactor activity involves residues situated in SCR-2 and SCR-4.

Because SCR-2 appeared to be the most important SCR for these activities, we next examined the individual amino acids involved in SPICE-C3b interaction and activity within SCR-2 by making individual residue changes. We expressed the single-amino-acid substitutions in SCR-2 (Q77H, H98Y, S103Y, E108K, or E120K) and evaluated this panel of proteins for their C3b-binding and their ability to inhibit complement activation through the alternative pathway. All five proteins with single-residue substitutions showed 10-times higher binding to C3b than VCP. Each mutated protein had 11- to 87-fold enhanced inhibition of the alternative pathway than VCP. The activity we found correlated with the predictions formed by electrostatic modeling. It had similar activity with SPICE at inhibiting the alternative pathway. The amount needed for this inhibition was only 3-times less than SPICE.

Based on predictions from the electrostatic calculations of VCP, we made a double residue substitution in VCP SCR-2 (E108K and E120K), which had generated a similar electrostatic profile contained in SPICE (Fig. 4). We predicted that a protein with these two residue changes would display many of the same properties that the 11 residue changes contained in SPICE. The recombinant VCP-E108K/E120K mutant resulted in a protein with increased complement regulatory activity. It had similar activity with SPICE at inhibiting the alternative pathway activation. The amount needed for this inhibition was only 3-times less than SPICE. It also had cofactor activity similar to SPICE.

It appears that electrostatic interactions are a property of other RCAs containing SCRs. Earlier studies have shown that the recognition between C3d and CR2(SCR-1/SCR-2) is electrostatic in nature involving macrodipoles through the volumes of C3d and CR2(SCR-1/SCR-2) (31). A two-step association model was proposed for C3d-CR2(SCR-1/SCR-2). The first step involved long-range electro-static interactions, while the second step involved local structural rearrangements to achieve shape and physico-chemical complementarity and to facilitate docking (31). The shape complementarity involved local van der Waals interactions. The physico-chemical complementarity involved local hydrophobic interactions and local electrostatic interactions in the form of hydrogen bonds and salt bridges.

Our data demonstrate how the 11 residue differences between SPICE and VCP result in such enhanced function. The multilog$_{10}$ increase in the complement regulatory activity of SPICE when compared with VCP permitted the systematic study of the domains and amino acid changes that contributed to this enhanced activity predicted by electrostatic modeling. Our data validates an electro-static model of interaction between SCR-containing proteins and C3b. That is, a predominantly negative C3b and a predominantly positive VCP variant favor

their electrostatically driven recognition and enhance their association. Increase in the positive charge of VCP variants occurs by mutations of acidic amino acids, which reduce the negative character of the electrostatic potential at the vicinity of SCR-2 and SCR-3 and enhance the positive character of the electrostatic potential at SCR-1 and SCR-4. This model has important implications in both our understanding of how RCA interact with C3b and the rational design of potent complement inhibitors that might be used as therapeutic agents (38, 39).

Acknowledgments

We thank R. B. Sim and S. A. Tsiftsoglou (University of Oxford) for providing factor I, W. DeGrado (University of Pennsylvania) for allowing limitless access to his spectropolarimeter, E. Ampatzi for assistance with the mass spectrometry, and D. McCellan for editorial assistance.

References

1. Liszewski, MK.; Atkinson, JP. Regulatory proteins of complement. In: Volanakis, JE.; Frank, MM., editors. The Human Complement System in Health and Disease. Decker; New York: 1998. p. 149
2. Hourcade D, Liszewski MK, Krych-Goldberg M, Atkinson JP. Functional domains, structural variations and pathogen interactions of MCP, DAF and CR1. Immunopharmacology. 2000; 49(103)
3. Herbert A, O'Leary J, Krych-Goldberg M, Atkinson JP, Barlow PN. Three-dimensional structure and flexibility of proteins of the RCA family—a progress report. Biochem Soc Trans. 2002; 30:990. [PubMed: 12440959]
4. Mastellos D, Morikis D, Isaacs SN, Holland MC, Strey CW, Lambris JD. Complement: structure, functions, evolution, and viral molecular mimicry. Immunol Res. 2003; 27:367. [PubMed: 12857982]
5. Mullick J, Kadam A, Sahu A. Herpes and pox viral complement control proteins: “the mask of self”. Trends Immunol. 2003; 24:24.
6. Blue CE, Spiller OB, Blackbourn DJ. The relevance of complement to virus biology. Virology. 2004; 319:319.
7. Uvarova EA, Shchelkunov SN. Species-specific differences in the structure of orthopoxvirus complement-binding protein. Virus Res. 2001; 81:81.
8. Kotwal GJ, Moss B. Vaccinia virus encodes a secretory polypeptide structurally related to complement control proteins. Nature. 1988; 335:335.
9. Kotwal GJ, Isaacs SN, McKenzie R, Frank MM, Moss B. Inhibition of the complement cascade by the major secretory protein of vaccinia virus. Science. 1990; 250:250.
10. Isaacs SN, Kotwal GJ, Moss B. Vaccinia virus complement-control protein prevents antibody-dependent complement-enhanced neutralization of infectivity and contributes to virulence. Proc Natl Acad Sci USA. 1992; 89:89. [PubMed: 1729724]
11. McKenzie R, Kotwal GJ, Moss B, Hammer CH, Frank MM. Regulation of complement activity by vaccinia virus complement-control protein. J Infect Dis. 1992; 166:166.
12. Sahu A, Isaacs SN, Soulika AM, Lambris JD. Interaction of vaccinia virus complement control protein with human complement proteins: factor I-mediated degradation of C3b to iC3b1 inactivates the alternative complement pathway. J Immunol. 1998; 160:160.
13. Rosengard AM, Alonso LC, Korb LC, Baldwin WM III, Sanfilippo F, Turka LA, Ahearn JM. Functional characterization of soluble and membrane-bound forms of vaccinia virus complement control protein (VCP). Mol Immunol. 1999; 36:36.
14. Bernet J, Mullick J, Panse Y, Parab PB, Sahu A. Kinetic analysis of the interactions between vaccinia virus complement control protein and human complement proteins C3b and C4b. J Virol. 2004; 78:78.
15. Smith SA, Sreenivasan R, Krishnasamy G, Judge KW, Murthy KH, Arjunwadkar SJ, Pugh DR, Kotwal GJ. Mapping of regions within the vaccinia virus complement control protein involved in

dose-dependent binding to key complement components and heparin using surface plasmon resonance. Biochim Biophys Acta. 2003; 1650:1650.

16. Wiles AP, Shaw G, Bright J, Perczel A, Campbell ID, Barlow PN. NMR studies of a viral protein that mimics the regulators of complement activation. J Mol Biol. 1997; 272:272.
17. Kirkitadze MD, Henderson C, Price NC, Kelly SM, Mullin NP, Parkinson J, Dryden DT, Barlow PN. Central modules of the vaccinia virus complement control protein are not in extensive contact. Biochem J. 1999; 344:344.
18. Henderson CE, Bromek K, Mullin NP, Smith BO, Uhrin D, Barlow PN. Solution structure and dynamics of the central CCP module pair of a poxvirus complement control protein. J Mol Biol. 2001; 307:307.
19. Murthy KH, Smith SA, Ganesh VK, Judge KW, Mullin N, Barlow PN, Ogata CM, Kotwal GJ. Crystal structure of a complement control protein that regulates both pathways of complement activation and binds heparan sulfate proteoglycans. Cell. 2001; 104:104.
20. Ganesh VK, Smith SA, Kotwal GJ, Murthy KH. Structure of vaccinia complement protein in complex with heparin and potential implications for complement regulation. Proc Natl Acad Sci USA. 2004; 101:101.
21. Rosengard AM, Liu Y, Nie Z, Jimenez R. Variola virus immune evasion design: expression of a highly efficient inhibitor of human complement. Proc Natl Acad Sci USA. 2002; 99:99.
22. Kotwal GJ, Moss B. Analysis of a large cluster of nonessential genes deleted from a vaccinia virus terminal transposition mutant. Virology. 1988; 167:167.
23. Dodd I, Mossakowska DE, Camilleri P, Haran M, Hensley P, Lawlor EJ, McBay DL, Pindar W, Smith RA. Overexpression in *Escherichia coli*, folding, purification, and characterization of the first three short consensus repeat modules of human complement receptor type 1. Protein Expression Purif. 1995; 6:727.
24. Kraus D, Medof ME, Mold C. Complementary recognition of alternative pathway activators by decay-accelerating factor and factor H. Infect Immun. 1998; 66:66.
25. Sarrias MR, Franchini S, Canziani G, Argyropoulos E, Moore WT, Sahu A, Lambris JD. Kinetic analysis of the interactions of complement receptor 2 (CR2, CD21) with its ligands C3d, iC3b, and the EBV glycoprotein gp350/220. J Immunol. 2001; 167:167.
26. Guex N, Peitsch MC. SWISS-MODEL and the Swiss-PdbViewer: an environment for comparative protein modeling. Electrophoresis. 1997; 18:18.
27. Berman HM, Westbrook J, Feng Z, Gilliland G, Bhat TN, Weissig H, Shindyalov IN, Bourne PE. The Protein Data Bank. Nucleic Acids Res. 2000; 28:28.
28. Lobley A, Whitmore L, Wallace BA. DICHROWEB: an interactive website for the analysis of protein secondary structure from circular dichroism spectra. Bioinformatics. 2002; 18:18.
29. Whitmore L, Wallace BA. DICHROWEB, an online server for protein secondary structure analyses from circular dichroism spectroscopic data. Nucleic Acids Res. 2004; 32:W668. [PubMed: 15215473]
30. Sahu A, Isaacs SN, Lambris JD. Modulation of complement by recombinant vaccinia virus complement control protein. Mol Immunol. 1996; 33:33. [PubMed: 8604222]
31. Morikis D, Lambris JD. The electrostatic nature of C3d-complement receptor 2 association. J Immunol. 2004; 172:172.
32. Ross GD, Lambris JD, Cain JA, Newman SL. Generation of three different fragments of bound C3 with purified factor I or serum. I. Requirements for factor H vs CR1 cofactor activity. J Immunol. 1982; 129:129.
33. Ross GD, Newman SL, Lambris JD, Devery-Pocius JE, Cain JA, Lachmann PJ. Generation of three different fragments of bound C3 with purified factor I or serum. II. Location of binding sites in the C3 fragments for factors B and H, complement receptors, and bovine conglutinin. J Exp Med. 1983; 158:158.
34. Spiller OB, Blackbourn DJ, Mark L, Proctor DG, Blom AM. Functional activity of the complement regulator encoded by Kaposi's sarcoma-associated herpesvirus. J Biol Chem. 2003; 278:278.

35. Mark L, Lee WH, Spiller OB, Proctor D, Blackbourn DJ, Villoutreix BO, Blom AM. KSHV complement control protein mimics human molecular mechanisms for inhibition of the complement system. J Biol Chem. 2004; 10:10.

36. Fukui A, Yuasa-Nakagawa T, Murakami Y, Funami K, Kishi N, Matsuda T, Fujita T, Seya T, Nagasawa S. Mapping of the sites responsible for factor I-cofactor activity for cleavage of C3b and C4b on human C4b-binding protein (C4bp) by deletion mutagenesis. J Biochem. 2002; 132:132.

37. Krych M, Hauhart R, Atkinson JP. Structure-function analysis of the active sites of complement receptor type 1. J Biol Chem. 1998; 273:273.

38. Mizuno M, Morgan BP. The possibilities and pitfalls for anti-complement therapies in inflammatory diseases. Curr Drug Targets Inflamm Allergy. 2004; 3:3.

39. Acosta J, Qin X, Halperin J. Complement and complement regulatory proteins as potential molecular targets for vascular diseases. Curr Pharm Des. 2004; 10:203. [PubMed: 14754399]

A

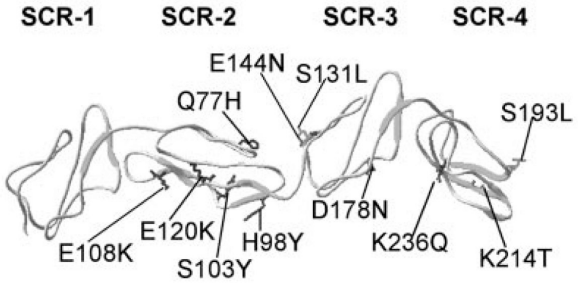

B

		SCR2					SCR3			SCR4		
#	Name	Q77H	H98Y	S103Y	E108K	E120K	S131L	E144N	D178N	S193L	K214T	L236Q
1	VCP											
2	SPICE	+	+	+	+	+	+	+	+	+	+	+
3	VCP-SPICE2	+	+	+	+	+						
4	VCP-SPICE3						+	+	+			
5	VCP-SPICE4									+	+	+
6	VCP-SPICE2-3	+	+	+	+	+	+	+	+			
7	VCP-SPICE2-4	+	+	+	+	+				+	+	+
8	VCP-SPICE3-4						+	+	+	+	+	+
9	VCP-Q77H	+										
10	VCP-H98Y		+									
11	VCP-S103Y			+								
12	VCP-E108K				+							
13	VCP-E120K					+						
14	VCP-E108K/E120K				+	+						

Figure 1.

Residue differences between VCP and SPICE *A*, Ribbon representation of the modeled structure of SPICE with stick representation of the 11 mutations of SPICE relative to VCP. The structure of SPICE was modeled using chain A of the VCP structure with PDB code 1g40. The SCR modules and the mutations are marked in the figure *B*, VCP-mutants expressed in *E. coli*. The first letter represents the VCP amino acid; the number indicates the amino acid position; and the second letter indicates the SPICE amino acid.

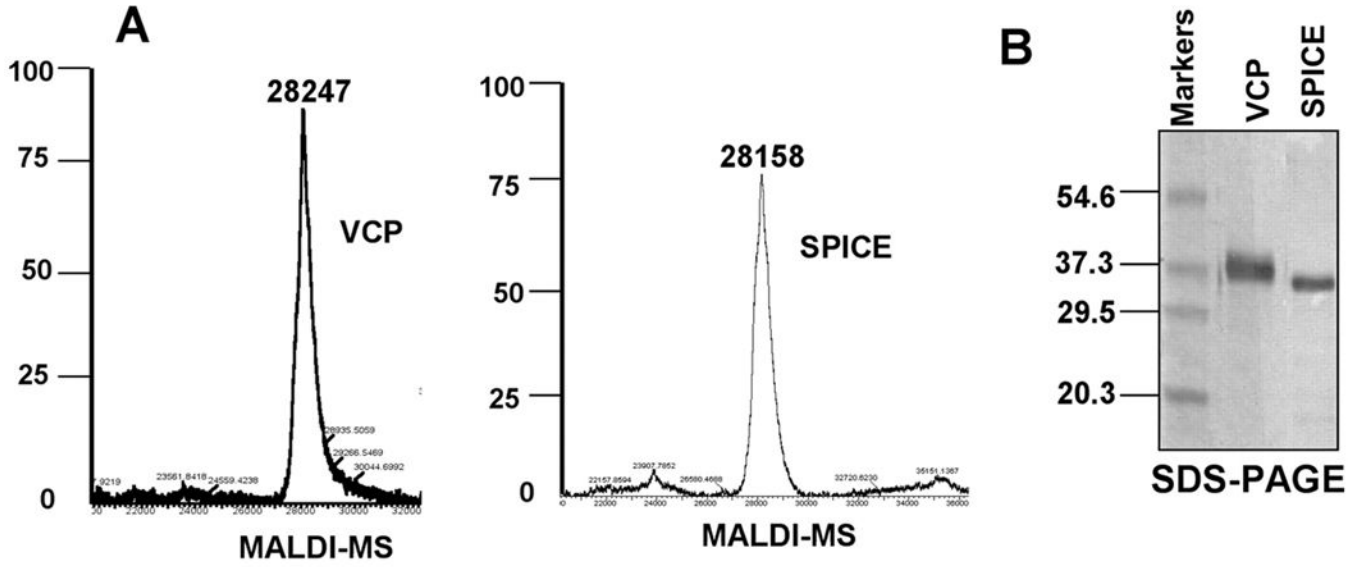

C

	Helix 1	Helix 2	Strand 1	Strand 2	Tums	Unordered	Total
VCP	-0.01	0.07	0.26	0.14	0.19	0.34	0.99
SPICE	0.02	0.08	0.22	0.13	0.22	0.33	1
VCP-SPICE 2	0	0.04	0.21	0.16	0.22	0.37	1
VCP-E108K/E120K	-0.01	0.06	0.21	0.12	0.23	0.37	0.98

Figure 2.

Biochemical characterization of VCP and SPICE. A, Mass spectrometric analysis of VCP (*left panel*) and SPICE (*right panel*) B, Coomassie-stained 10% SDS-PAGE gel showing VCP and SPICE under reducing conditions. Numbers on the *left* indicate the molecular mass in kilodaltons of mass markers *C*, CD analysis of the proteins. Secondary structure composition calculated by deconvoluting the spectra using the CDSSTR algorithm, which is a part of the web based CD analysis tool DICHROWEB (28, 29).

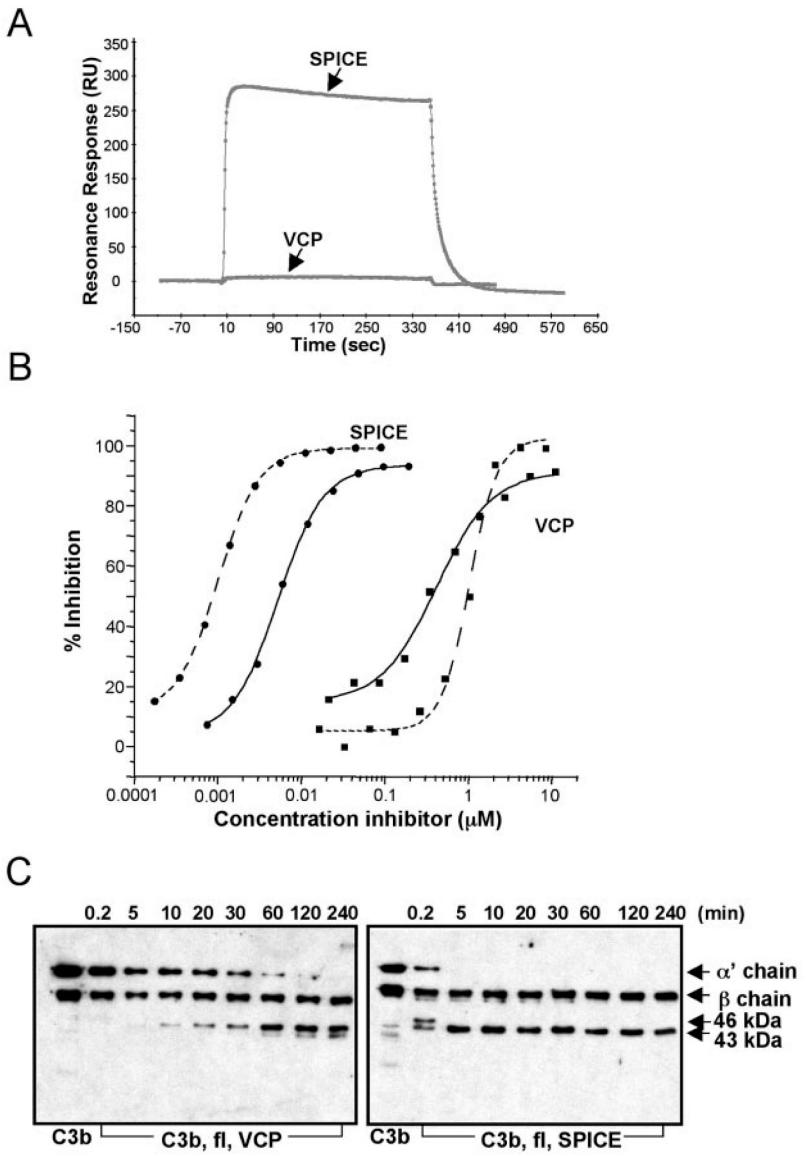

Figure 3.

Complement modulating activity of VCP and SPICE. *A*, Binding of SPICE and VCP to human C3b by SPR. SPR experiments were conducted using an SA chip where biotinylated C3b was immobilized. Solutions of SPICE and VCP (each 50 nM) were passed through with a flow of 10 μl/min. After injection of the protein (360 s), SPR was followed for an additional 200 s. The response during the time is expressed in resonance response units (RU). *B*, Inhibition of complement activation. The deposition of human C3b in the presence of various amounts of SPICE and VCP on an immunocomplex (classical pathway) or on LPS (alternative pathway) was detected using a polyclonal anti-C3b Ab. The results are expressed as the percent inhibition of complement activation. The solid lines indicate the classical pathway, and the dashed lines indicate the alternative pathway *C*, Factor I cofactor activity of VCP and SPICE. VCP and SPICE (300 ng) were incubated with C3b (500 ng) in the presence of factor I (fI, 10 ng). Samples were collected at indicated time points and were

subjected to Western blot analysis. For the detection of the degradation products of C3b, a polyclonal anti-C3b Ab was used. The appearance of the 46 kDa and the 43 kDa indicate the generation of the $iC3b_1$ and $iC3b_2$, respectively.

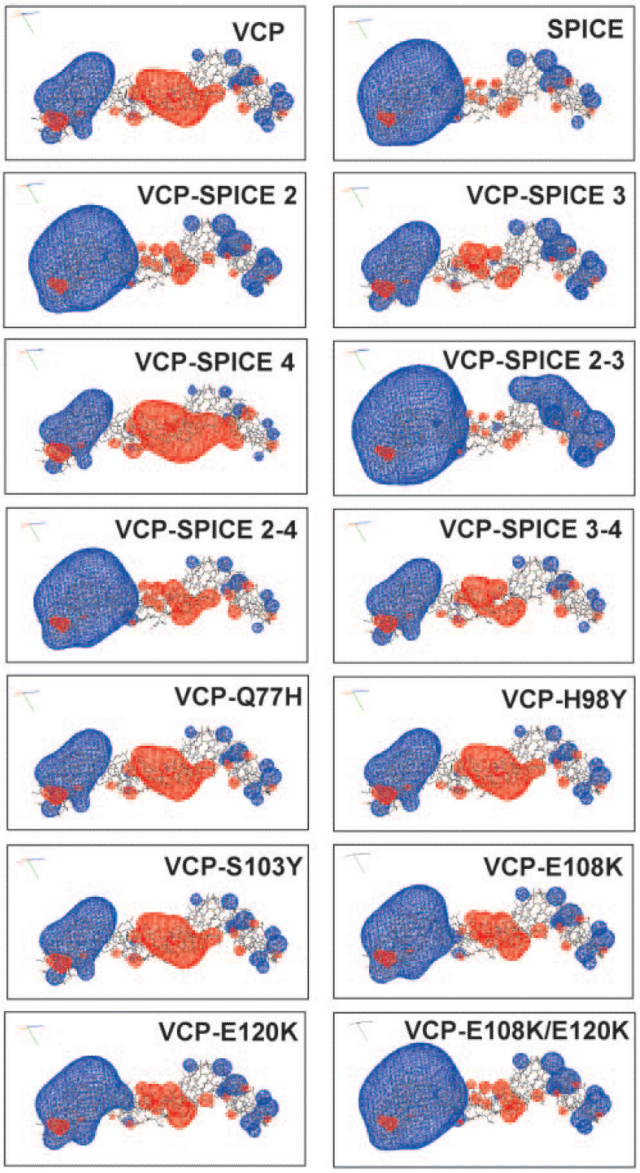

Figure 4.

Iso-potential contour surfaces for native VCP and several theoretical mutants of VCP including SPICE. Blue and red denote positive and negative electrostatic potential, respectively. The structure of VCP with PDB Code 1g40 (19) was used to construct the structures of SPICE and theoretical mutants. The coordinates of all mutants were fit to the coordinates of native VCP using the backbone Cα atoms. The orientation of the structures and the electrostatic potential calculations were performed using the same parameters for all panels. Modeling was performed using the program Swiss-PdbViewer (26).

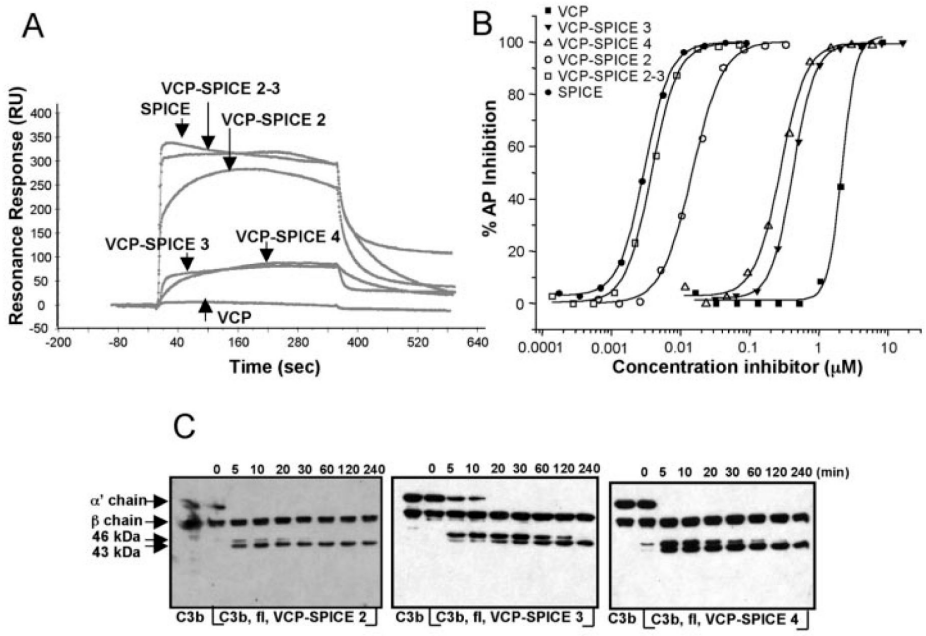

Figure 5.

Mapping of SPICE SCRs involved in the enhanced interaction of SPICE with C3b *A*, Binding of VCP-SPICE mutants to immobilized C3b. The experiment was conducted as described in Fig. 3A. *B*, Inhibition of alternative pathway by VCP-SPICE variants. The experiment was conducted as described in Fig. 3B. *C*, factor I (fI) cofactor activity of VCP-SPICE mutants. Recombinant proteins were incubated with C3b in the presence of fI and analyzed as described in Fig. 3C.

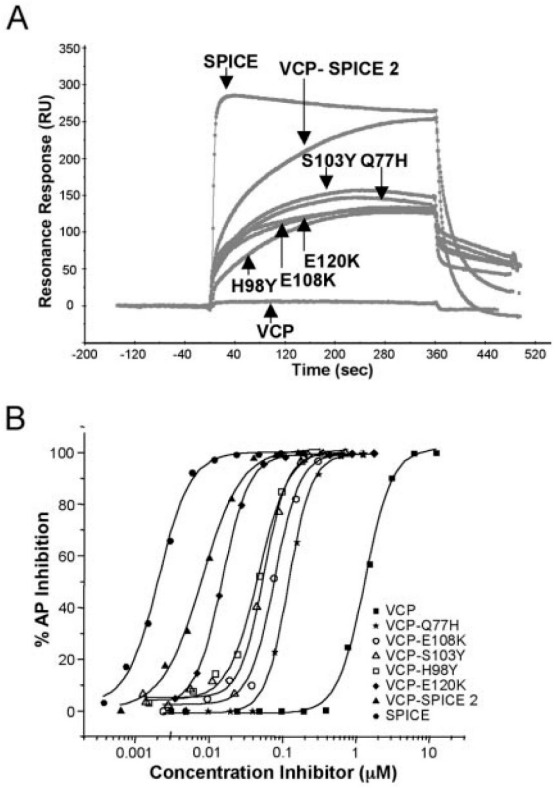

Figure 6.

Mapping of the activity of SPICE by single mutations in SCR-2. *A*, Analysis of the binding of VCP-SPICE variants to immobilized C3b. The letters and numbers above each arrow represent the individual residue changes in VCP summarized in Fig. 1B. The experiment was conducted as it is described in Fig. 3A. *B*, Inhibition of alternative pathway complement activation by VCP-SPICE mutants. The experiment was conducted as described previously in Fig. 3B.

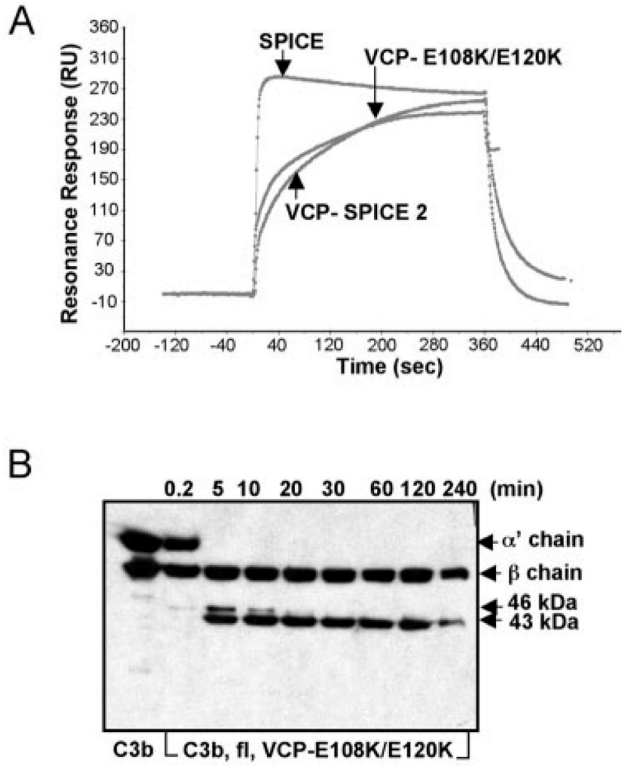

Figure 7.

Mapping of the activity of SPICE by mutating positions E108K and E120K on VCP. *A*, Binding of VCP variants to immobilized C3b. The experiment was conducted as it is described in Fig. 3A. *B*, factor I cofactor activity of VCP-E108K/E120K. The experiment was performed as described in Fig. 3C.